

# A Hardware Platform for Tuning of MEMS Devices Using Closed-Loop Frequency Response

Michael I. Ferguson, Didier Keymeulen, Ken Hayworth, Brent Blaes, Chris Peay, Karl Yee,  
Jet Propulsion Laboratory,  
(Corresponding) Michael.I.Ferguson@jpl.nasa.gov  
MS 303/300, 4800 Oak Grove Dr., Pasadena, CA 91109, 818-393-6967

Eric MacDonald – University of Texas at El Paso,  
500 West University Dr., El Paso, TX 79968-0523, 915-747-5969

David Foor – Texas A&M – Kingsville,  
719 W Kleberg, Kingsville, TX 78363, 361-549-6338.

**Abstract**—We report on the development of a hardware platform for integrated tuning and closed-loop operation of MEMS gyroscopes. The platform was developed and tested for the second generation JPL/Boeing Post-Resonator MEMS gyroscope. The control of this device is implemented through a digital design on a Field Programmable Gate Array (FPGA). A software interface allows the user to configure, calibrate, and tune the bias voltages on the microgyro. The interface easily transitions to an embedded solution that allows for the miniaturization of the system to a single chip.<sup>12</sup>

## TABLE OF CONTENTS

<b>1. INTRODUCTION.....</b>	<b>1</b>
<b>2. MECHANICS OF THE MEMS MICROGYRO.....</b>	<b>2</b>
<b>3. CONTROL OF THE MICROGYRO.....</b>	<b>3</b>
<b>4. GYRO DIGITAL SUBSYSTEM.....</b>	<b>4</b>
<b>5. RESULTS AND FUTURE MODIFICATIONS .....</b>	<b>4</b>
<b>6. SUMMARY AND DISCUSSION.....</b>	<b>5</b>
<b>7. ACKNOWLEDGEMENTS .....</b>	<b>6</b>
<b>REFERENCES .....</b>	<b>6</b>
<b>BIOGRAPHY .....</b>	<b>6</b>

## 1. INTRODUCTION

The JPL/Boeing MEMS post resonator gyroscope (PRG), is a MEMS analogue to the classical Foucault pendulum. A Pyrex post anodically bonded to a silicon plate is driven into a rocking mode by sinusoidal actuation via electrodes beneath the plate. In a rotating reference frame the post is coupled to the Coriolis force, which exerts a tangential “force” on the post. Another set of electrodes beneath the device sense this component of motion. The voltage that is required to null out this motion out is directly proportional to the rate of rotation to which the device is subjected.

All gyroscopes suffer from performance limitations due to bias instabilities which result in zero-rate drift. The PRG has demonstrated an in-run bias stability of 0.1 deg/hr, roughly an order of magnitude better than that of other competing MEMS-based gyroscopes, and is comparable in performance to optical gyroscopes. Other designs such as spinning-mass gyroscopes are typically orders of magnitude larger, more massive, and power consumptive, so there is a great incentive among the aerospace community to develop lighter, more compact and power efficient gyroscopes. Optical gyroscopes such as Fiber Optic Gyros (FOGs) and Ring Laser Gyros (RLGs) are also large, power consumptive and expensive; in addition, FOGs suffer performance degradation when exposed to radiation due to optical fiber darkening, while RLGs suffer from laser life issues. This adds incentive to develop the MEMS devices in order to produce a navigation-grade gyroscope for spaceflight with the form-factor available with these devices. The end result of using the microgyro in these non-conventional environments will reduce size, mass and power while maintaining control of the remote system. Typical applications that would benefit from this technology include: inertial spacecraft navigation to complement a star tracker or sun sensor, integration of the device in a planetary rover or lunar or planetary sample return missions that have a premium on weight because of the cost of lifting mass off the remote surface, the detection of angular rotation in all axes of a robotic arm

As a corollary to the advancement of technology, new control systems must be developed to interface to the small structures each tailored to the particular system a few are listed here [2]-[5]. The PRG structure suffers, before tuning, from a decrease in sensitivity due to the two dimensional resonant structure being non-degenerate. This is a result of manufacturing imprecision that leads to asymmetry in the silicon structure. This will be explained further in Section 2. The result of the inherent asymmetry results in the existence of a non-degeneracy in the modes along the two modal axes.

<sup>1</sup> 0-7803-8870-4/05/\$20.00©2005 IEEE

<sup>2</sup> IEEEAC paper #1284, Version 4, Updated January 10, 2005

Two general solutions exist for the problem of decreased sensitivity. (1) By increasing the accuracy in the manufacturing process, the microgyro will be more symmetric. This, however, would be expensive and impractical in light of another solution. (2) Corrections can be applied to the system post-fabrication. The corrections are far more cost effective and take several forms. One form of correction is to apply a transformation to the vibration for both axes of rotation [6]. Unfortunately this correction method requires a careful characterization of the covariance matrix, which is a numeric measurement of the coupling between the X- and Y-axes. Another form of correction is to adapt the resonant frequency of the gyroscope by applying feedback, a closed-loop approach [7]. A third form of correction is to change the sensing pickoff frame by creating weighted sums of the pickoff signals to decouple the dynamics [8]. The third form of correction also allows for a further improvement in the decoupling of the axes by using electrostatic biasing forces to modify the spring constants of the vibratory system. As the modes of oscillation become degenerate, sensitivity increases regardless of the device's inherent asymmetry. By calibrating the device to force the case of degenerate oscillation modes, an Inertial Measurement Unit (IMU) of comparable sensitivity to the spinning-mass variety can be achieved.

This paper presents the design and implementation of a control system to implement the electrostatic biasing approach described above. The principle of electrostatic biasing is based on measuring the resonance frequencies of the drive axis at a given set of bias voltage then swapping and driving the other axis, thereby extracting the resonant frequency of both axes. An algorithm is then applied iteratively to modify the bias voltages until the resonant frequency of each axis is equal. A major advantage of this approach is that the resonant frequencies can be extracted quickly (~1 second) as compared with the open-loop control system, which takes two orders of magnitude longer. The effect of balancing using this approach can be seen in a reduced asymmetrical rate bias.

The design of the electrostatic approach is realized on an FPGA with augmented portability for future designs and implementations. This paper is organized such that Section 2 describes the mechanics of the microgyro, Section 3 describes the control system, Section 4 describes the Gyro Digital Subsystem and the results of our preliminary experiments, Section 5 describes future directions and Section 6 summarizes the project results.

## 2. MECHANICS OF THE MEMS MICROGYRO

The mechanical design of the microgyro can be seen in Figure 2. In order for the gyroscope to operate, the Pyrex posts (center) must vibrate along an axis (i.e. X as labeled in

the figure). Because the oscillations are driven on this axis, it is called the drive axis. Rotation  $\Omega$  around the Z-axis will cause coriolis forces that couple vibrations from the drive axis to the orthogonal axis, called the sense axis (i.e. Y as labeled in the figure). The vibrations coupled to this sense axes are related to the angular rate  $\Omega$  of rotation along the Z-axis. Pyrex posts are anodically bonded to the top and bottom of the upper silicon plate (i.e. the resonator), which is eutically bonded to an electrical baseplate via four torsional springs. Atop the electrical baseplate are 16 capacitive petals used for electrostatic spring softening and driving and sensing the motion of the resonator. The upper and lower plates are set 20 $\mu$ m apart. Oscillations cause a variation of capacitance to occur in the internal structure of the device. This change in capacitance generates a time-varying sinusoidal charge that can be converted to a voltage using the relationship,  $V=Q/C$ . The post can be driven around the drive axis by applying a time-varying voltage signal to the drive electrodes labeled D1-, D1+, D1in- and D1in+ in Figure 2. Because there is symmetry in the device, either of the two axes can be designated as the drive axis. Each axis has a capacitive electrode pair for sensing oscillations (labeled S1+ and S1- in Figure 2) and a driving electrode pair (labeled D1in+ and D1in- in Figure 2. The microgyro has additional plates that allow for electro-static spring-softening and damping labeled B1, BT1, B2, and BT2 in Figure 2. Static bias voltages can be used to modify the amount of damping to each oscillation mode. In an ideal symmetric device the resonant frequencies of both modes are equal; however, manufacturing imperfections in the machining of the device can cause asymmetries in the devices silicon structure. This results in asymmetry of the vibration modes. This can arise from several different places in the fabrication process. One reason asymmetries between the oscillation modes exists is due to imperfect lithography. Because the etching of the silicon is very temperature dependent, imperfect etching can result when temperature gradients form across the silicon wafer. Another reason for the asymmetry is due to the alignment of the top plates to the baseplate. Also, the bonding of the Pyrex posts can cause an inconsistency in the modes of oscillation because the posts need to be aligned with respect to the resonator, baseplate and each other. Because of these imperfections, non-degeneracy in the post's modes of oscillation exists, which manifests as a difference in the resonant frequencies along each. The frequency split reduces the mechanical coupling between the two modal axes. By adjusting the static bias voltages on the capacitor, both harmonics are modified to match each other; this is referred to as the tuning of the device.

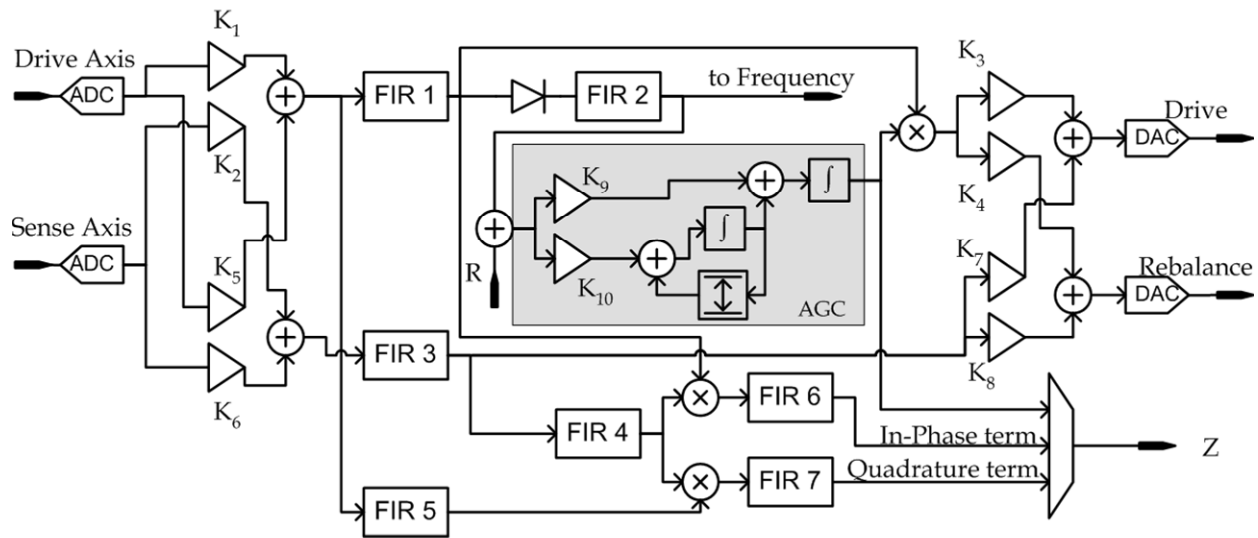


Figure 1. A schematic of the Closed-Loop Control System.

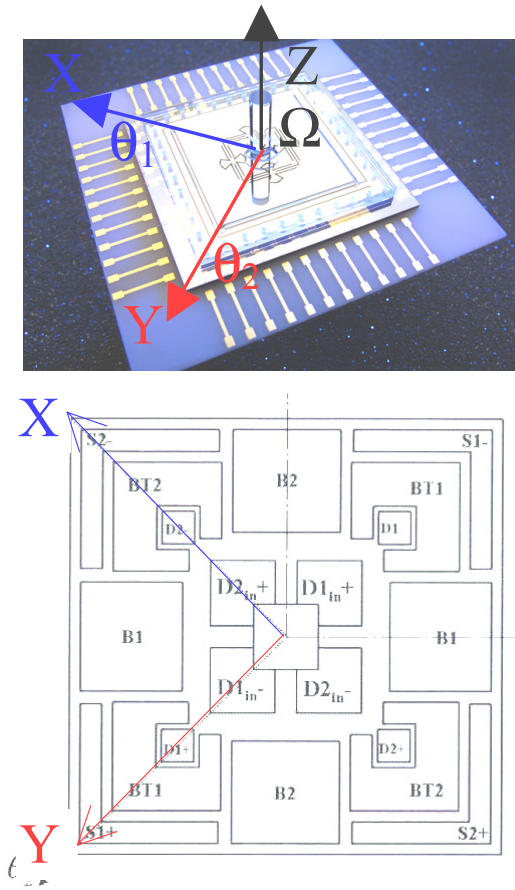


Figure 2. A magnified picture of the JPL microgyro with sense axis Y (S2-, S2+ electrodes used to sense, D2-, D2+, D2in- and D2in+ used to drive along the sense axis) and drive axis X (D1-, D1+, D1in- and D1in+ used to drive, S1-, S1+ electrodes used to sense along the drive axis) and the electrodes used for biasing (B1, B2, BT1, BT2) (picture courtesy of C. Peay, JPL).

### 3. CONTROL OF THE MICROGYRO

As mentioned above, coriolis forces act on the oscillating Pyrex post causing the plane of oscillation to rotate about the Z-axis and is passed to the two degree-of-freedom rocking motion of the plate parameterized by the  $\theta_1$  and  $\theta_2$  angular coordinates along drive axis X and sense axis Y. The control system detects this rotation by sensing motion around the sense axis. Since the amount of rotation is related to the angular momentum sensed in the “sense” direction, the torque required to null out that motion is again related to the rotation. This process is called sense rebalancing and the amount of torque needed to rebalance is quantified as an amount of angular rotation. If the relationship between the sense and drive axes is non-linear, the resultant torque applied to rebalance the oscillations will also yield a non-linear quantification of the angular rate. As noted previously, modifying the static bias voltages to cause changes in the spring constants for both axes allows for a closer linear relationship to exist between the vibration modes. In order to extract the resonant frequencies of the vibration modes, there are two general methods, 1) open-loop and 2) closed-loop control. In an open-loop system, we are measuring the frequency response along the drive axis over 50Hz band. The measurement consists of exciting the drive axis with a sine wave at a given frequency and measuring the resulting amplitude. This is done repeatedly through the frequency spectrum. Because of cross coupling between the different axes, two peaks in the amplitude response will appear at two different frequencies, showing the resonant frequencies of both modes. This takes approximately 1.4 minutes to complete and must be done at least three times to average out noise. A faster implementation is a close-loop control whereby the gyro is given an impulse disturbance and allowed to oscillate freely. This so-called “pinging” of the vibration mode

allows the gyroscope to immediately settle to its natural frequency. The corresponding frequency,  $F_1$ , is measured from the sensing plate under the drive axis X. Because the device is relatively symmetric, the drive and sense axes are swapped and the other mode is pinged to get  $F_2$ . The difference in the frequencies is determined in about 1.5 seconds, which is roughly 50 times faster than from the open-loop control method. This ability to quickly swap the drive axis with the sense axis is a feature of our Gyro Digital Subsystem (GDS) and will be tested in our future experiments.

A schematic of the closed-loop control system can be seen in Figure 1. This circuitry includes a drive loop and a sense rebalance loop. The drive loop takes the input from the “drive-sense” electrodes along the drive axis ( $S1-$ ,  $S1+$ ), and outputs the forcing signal to the “drive drive” electrodes along the drive axis ( $D1-$ ,  $D1+$ ,  $D1in-$  and  $D1in+$ ). The sense rebalance loop receives input from the “sense sense” electrodes along the sense axis ( $S2-$ ,  $S2+$ ), and forces, or rebalances, the oscillations back along the drive axis with a forcing signal to the “sense drive” ( $D2-$ ,  $D2+$ ,  $D2in-$  and  $D2in+$  electrodes). The magnitude of this forcing function in the rebalance loop is related to the angular rate of rotation. In Figure 1 there are several scaling coefficients indicated  $K_i$ , where  $i$  ranges from 1 to 10. These constants allow for a mixing of the sensed signals from both axes as described in [8] and allows for a *virtual* drive axis anywhere through a full 360 degrees. We augment the use of these constants by using them to swap the meaning of the drive- and sense-axis, so that the bulk of the energy switches between the two, thus allowing the tuning algorithm to measure the resonance frequency along the X- or Y-axis, or indeed any axis between X and Y [9].

Because the amplitude of the freely oscillating drive axis will naturally decay, another control task is implemented to lightly drive or damp, depending on circumstance, the drive axis so that the amplitude of the driven signal is constant. This feature is implemented through an Automatic Gain Control (AGC) loop, shown shaded in Figure 1 [8]. A signal rectification stage and proportional integrator loop are the main components of the AGC. The output of the AGC is a DC value that modulates the forcing function.

#### 4. GYRO DIGITAL SUBSYSTEM

The system used to implement the control, operation, and observability of the microgyro is referred to as the Gyro Digital Subsystem (GDS). Figure 3 illustrates the implementation of the analog and digital systems used to control the gyro. The key circuit elements that allow proper operation of the microgyro include the audio codec (Stereo Digital to Analog Converter DAC), high voltage Analog to Digital Converters (ADCs), IEEE-1284 Enhanced Parallel

Port (EPP) interface, and the Digital Signal Processor (DSP) functionality integrated into a Xilinx Virtex II FPGA.

The audio codec is used to translate the analog sensing signals for both the drive and sense axes. Its stereo capabilities allow for two inputs and two outputs. The high-voltage DACs are utilized for the setting of the static bias voltages on the gyroscope, which range from -15V to +60V. The parallel port interface allows for user input/output capabilities. The user can configure the coefficients for the finite impulse response (FIR) filters along with the scaling coefficients ( $K_1$  through  $K_8$ ) and PI coefficients ( $K_p$  and  $K_i$ ). The codec is configured through this interface as well.

The closed control loop design initially reported by other researchers [8] was improved with a graphical user interface (GUI). This interface allows the user to configure the ASIC and codec, change static voltage biases, and monitor outputs from critical areas within the closed control loop and the output from the demodulation stage, see Figure 5.

The utility of this new control system is realized by the ability to swap the drive signal between the X- and Y-axes for the extraction of the resonant frequencies. As mentioned above, in order to mitigate the mismatch in resonant frequencies the  $F_1$  and  $F_2$  should be equal. In practice this is never the case and a maximum error bound must be set in order for this source of error to be effectively removed. The error bound is determined as the point at which the zero-rate drift due to this source of error is zero. This had been determined empirically to be about 0.1Hz [10].

#### 5. RESULTS AND FUTURE MODIFICATIONS

The gyro was operated for a period of several hours and provided a frequency measurement that was stable to 1 mHz. A typical capture of the driving and sensed signals for the gyro is seen in Figure 4. In the figure, the signal Torque 2 is the drive signal along the sense Y Axis (rebalance signal in Figure 1). This signal was observed to be smaller during quiescent operation.

The existing system currently has a parallel interface to the host computer. This interface is currently being replaced with a serial interface toward the eventual goal of integrating the entire tuning and control package on a single device. In addition to the interface changes, a significant reduction in area, and power will be realized when we replace the 18-bit parallel multipliers and FIR filters currently used with combined units using online arithmetic [11]. This system has not yet been tested in the mode where the drive- and sense-axes are swapped, but based on our previous experiments using electrostatic tuning [12] this will be an effective tool to allow fast tuning of the gyro.

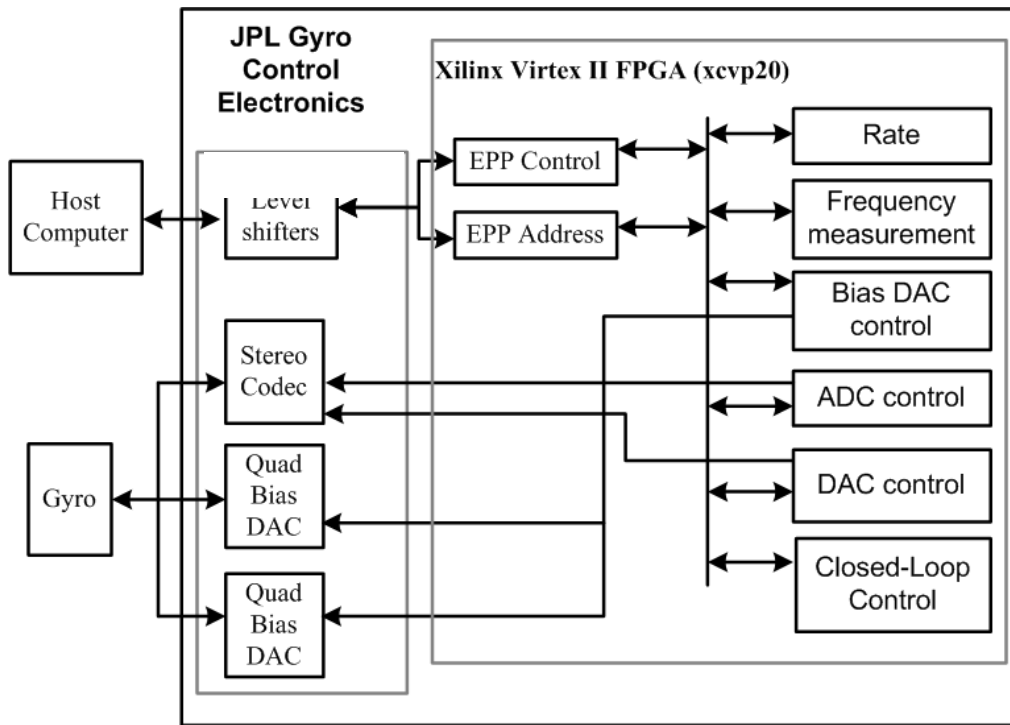


Figure 3. A block-diagram of the entire closed-loop control system.

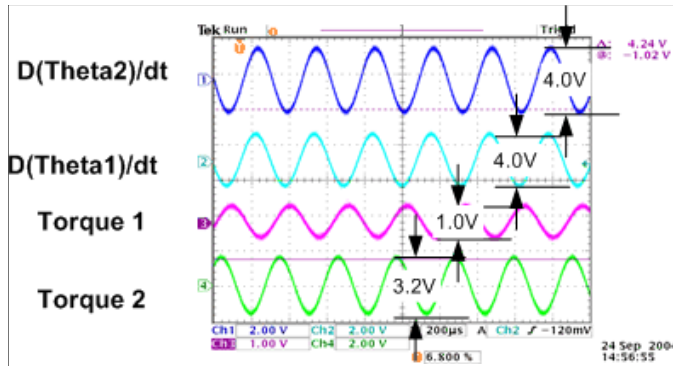


Figure 4. A typical set of waveforms for slight rotation around the Z-axis. The rebalance output (Torque 2 signal) can be seen so be approximately 3.2V.

## 6. SUMMARY AND DISCUSSION

The JPL/Boeing microgyro is a device that can be controlled and tuned by implementing an open- or closed-loop control digital system. This paper describes an option for the closed-loop system that has the option of swapping the drive- and sense-axes, thus decreasing the time required for tuning by more than a factor of fifty. The specific amount of rate bias reduction will be reported at a future date. Future design modifications will allow for even smaller control circuits by replacing the current 18-bit parallel multipliers and FIR filters by online modules, which routinely reduce the area significantly [11]. Additionally, a future design will include

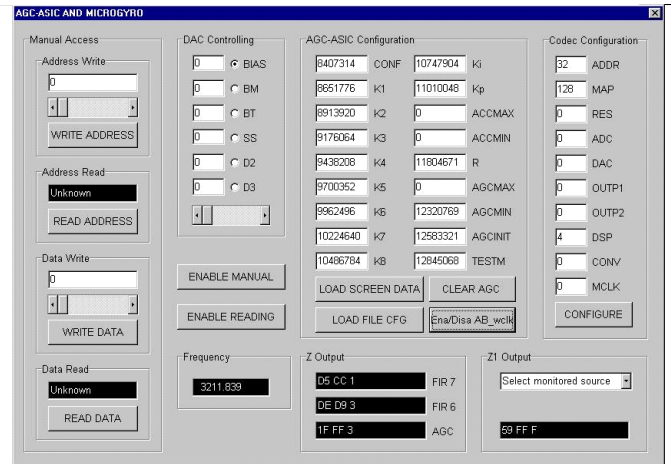


Figure 5. Graphical user interface to software used to program the closed-control loop GDS system.

an on-chip microprocessor to allow for in-situ re-tuning of the gyroscope in response to unexpected changes in the behavior due to radiation, aging, temperature effects or other faults. This automated tuning algorithm has been the focus of a parallel research effort [12]. In addition to tuning algorithm, another parallel effort is underway to model the effect of temperature on the performance of the gyroscope [13]. The combination of the intelligent tuning algorithm, a characterization of the temperature dependence and the closed-loop control system will lead to a robust, light-weight, low-power navigation-grade inertial measurement unit for use in space even in the most extreme environments.



## 7. ACKNOWLEDGEMENTS

The work described in this publication was carried out at the Jet Propulsion Laboratory, California Institute of Technology under a contract with the National Aeronautics and Space Administration. Leveraged funding was provided by NASA ESTO-CT, ARDA, and ONR. We also thank William M. Whitney for supporting David Foor under the Caltech - Summer undergraduate research fellowship program. A special thanks to Richard Terrile who has supported this research through the Research and Technology Development grant entitled "Evolutionary Computation Techniques for Space Systems" [14].

## REFERENCES

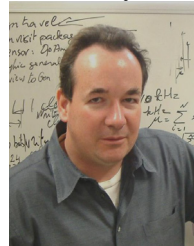
- [1] Lefevre, H.C., Bourbin Y., Graindorge P., Arditty H.J., "Review of fiber optic gyroscopes", *Proceedings of SPIE the international society for optical engineering* [0277-786X] Lefevre, yr: 1983 vol: 369 pg: 386.
- [2] R. P. Leland, "Lyapunov based adaptive control of a MEMS gyroscope," in Proc. 2002 Amer. Contr. Conf., Anchorage, AK, 2002, pp. 3765–3770.
- [3] S. Park, "Adaptive control strategies for MEMS gyroscopes," Ph.D. dissertation, Univ. California, Berkeley, 2000.
- [4] S. Park and R. Horowitz, "Adaptive control for Z-axis MEMS gyroscopes," in Proc. American Control Conf., Arlington, VA, June 25–27, 2001, pp. 1223–1228.
- [5] A. M. Shkel, R. Horowitz, A. A. Seshia, S. Park, and R. T. Howe, "Dynamics and control of micromachined gyroscopes," in Proc. American Control Conf., San Diego, CA, June 1999, pp. 2119–2124.
- [6] Painter C.C., Shkel A.M., "Active structural error suppression in MEMS vibratory rate integrating gyroscopes," *IEEE Sensors Journal*, vol.3, no.5, pp.595–606, Oct. 2003.
- [7] Leland, R.P., "Adaptive mode tuning for vibrational gyroscopes," *IEEE Trans. Control Systems Tech.*, vol.11, no.2, pp.242–7, March 2003.
- [8] Chen, Y. C., M'Closkey, R.T., Tran. T., Blaes. B., "A control and signal processing integrated circuit for the JPL-Boeing micromachined gyroscopes", to be published, 2004.
- [9] K. Hayworth, "Continuous Tuning and Calibration of Vibratory Gyroscopes", In NASA Tech Brief, Oct 2003 (NPO-30449)
- [10] Discussion with C. Peay.
- [11] M.D. Ercegovac and T. Lang, *Digital Arithmetic*, Morgan Kaufmann Publishers - An Imprint of Elsevier Science, 2004.
- [12] D. Keymeulen, W. Fink, M. Ferguson, C. Peay, B. Oks, K. Yee, "Tuning of MEMS device using Evolutionary Computation and open-loop Frequency Response Applied to the JPL MEMS microscopic gyro", in Proceedings of the IEEE Aerospace Conference, Big Sky, March 2005.
- [13] M. I. Ferguson, D. Keymeulen, C. Peay, K. Yee, D. Li, "Effect of Temperature on MEMS Vibratory Rate Gyroscope", in Proceedings of the IEEE Aerospace Conference, Big Sky, March 2005.
- [14] R. J. Terrile, et al., "Evolutionary Computation Technologies for Space Systems", in Proceedings of the IEEE Aerospace Conference, Big Sky, March 2005.

## BIOGRAPHY

**Michael I. Ferguson** is a member of the Technical Staff in the Bio-Inspired Technologies and Systems group. His focus is on evolutionary algorithm application to VLSI design and arithmetic algorithms. He is currently working on the application of GA to tuning MEMS micro gyros. His other projects include evolution of digital and analog circuits intrinsically and extrinsically using a variety of methods. He was the Local Chair of the 2003 NASA/DoD Conference on Evolvable Hardware. He received a M.S. in Computer Science from University of California at Los Angeles and a B.S. in Engineering Physics from the University of Arizona. Michael is a member of the IEEE.



**Didier Keymeulen** received the BSEE, MSEE and Ph.D. in Electrical Engineering and Computer Science from the Free University of Brussels, Belgium in 1994.. In 1995 he was the Belgium laureate of the Japan Society for the Promotion of Science Post Doctoral Fellowship for Foreign Researchers. In 1996 he joined the computer science division of the Japanese National Electrotechnical Laboratory as senior researcher. Since 1998, he is member of the technical staff of JPL in the Bio-Inspired Technologies Group. At JPL, he



is responsible for the applications of the DoD and NASA projects on evolvable hardware for adaptive computing that leads to the development of fault-tolerant electronics and autonomous and adaptive sensor technology. He served as the chair, co-chair, program-chair of the NASA/DoD Conference on Evolvable Hardware. Didier is a member of the IEEE.



**Kenneth Hayworth** has a BS in Computer Science and Engineering as well as a BS in Mathematics from the University of California at Los Angeles. During college, he worked as a research engineer for Ennex Fabrication Technologies designing and constructing prototype 3D object fabrication machines. After graduating,

he worked for over five years at the Jet Propulsion Laboratory as a research engineer developing MEMS gyroscopes for micro-spacecraft applications, as well as developing analog neural and evolvable electronic hardware. Ken is currently enrolled full time in the Neuroscience Graduate Program at the University of Southern California.

**Brent Blaes** received the B.S.E.E (77) and M.S.E.E. (79)



from California State Polytechnic Univ. Pomona and is presently a senior member of the engineering staff at NASA's Jet Propulsion Laboratory where he has 26 years experience in analog and digital circuit design, integrated circuit development, and

flight electronics. He has worked extensively in the development of test circuits, sensors and measurement techniques for characterizing total dose and SEU effects of CMOS circuits and in the development of magnetic mass-memory devices. He was the chief designer of the Radiation and Reliability Assurance Experiment (RRELAX) which flew on the Clementine-I spacecraft and the cognizant engineer and designer of the Free Flying Magnetometer (FFM) data system. He was the task manager for the New Millennium Programs DS2 Mars penetrator probe Follow-On-Experiment. He is currently leading the development of electronics for the external metrology system on NASA's Space Interferometry Mission (SIM).

**Chris Peay** is an Engineer affiliated with NASA's Jet Propulsion Laboratory. He is currently the electronics, control, and testing lead of the JPL MEMS gyroscope development team, which he has been part of for more than 2 years. Prior to joining the JPL gyro team, Chris gained 10 years experience in electronics and computer engineering, primarily in communications, software engineering, and semiconductors. He received the BS degree in Electrical Engineering



from the University of Utah and is pursuing the MSECE degree at the Georgia Institute of Technology.

**Karl Yee** received his Ph.D. in Theoretical Physics from the University of California, Irvine in 1994. He is a senior researcher within the MEMS Technology group at NASA's Jet Propulsion Laboratory, and has 14 years of experience working on space related projects as an electronic packaging engineer and as a MEMS engineer. He is currently the task manager of JPL's Miniature Gyroscope project.

**Eric MacDonald** received a BSEE, MSEE and PhDEE



from the University of Texas at Austin in 1992, 1997, and 2002 respectively. He has worked at IBM and Motorola doing circuit and logic design of processors and System-On-Chips (SOC) focusing on testability and ultra-low power design. In 2002, he co-founded a company Pleiades Design

and Test, Inc., which was acquired in 2003 by Magma Design Automation, Inc. In 2003, he joined the department of Electrical and Computer Engineering of the University of Texas at El Paso.

**David Foor** is working on his BSEE at Texas A&M –



Kingsville. As an undergraduate he received a summer research fellowship through the California Institute of Technology where he interned at the Jet Propulsion Laboratory. He is a member of the IEEE Robotics and Automation Society.